Spatially and Temporally Resolved Studies of Convectionless Photobleaching Kinetics: Line Trap†

Sung Hyun Park,‡,§ Hailin Peng,‡,§ Stephen Parus,‡,§ Haim Taitelbaum,#,§ and Raoul Kopelman*,‡

Department of Chemistry, University of Michigan, Ann Arbor, Michigan 48109-1055, and Department of Physics, Bar-Ilan University, Ramat-Gan 52900, Israel

Received: November 13, 2001; In Final Form: March 1, 2002

The kinetics of the growth of depletion zones around a static trap in an effective one-dimensional geometry were studied with a new fluorescence-based setup. The experiment consists of a photobleaching reaction of fluorescein dye by a strong laser beam, which served as a phototrap in the experiment, inside a 150-μm gap between two parallel microscope slides. The kinetics of the growth of the depletion zone were monitored by the previously defined θ distance, which can be directly measured experimentally. The effect of trap strengths on the kinetics was tested experimentally by changing the photobleaching laser power. The strong laser power acted as a perfect trap, which gives a $t^{1/2}$ scaling behavior for the θ distance over most of the time range. However, the experiment with a weak laser power produced an anomalous early-time behavior for the θ distance, which is faster than the $t^{1/2}$ time scaling. A crossover behavior was observed with an intermediate laser power. The experimental results are consistent with an exact one-dimensional analytical solution and were also reproduced in Monte Carlo simulations as well as by exact enumeration calculations. The latter two methods show that the asymptotic results for an exact one-dimensional lattice are still valid in a quasi-one-dimensional system, for both perfect and imperfect trapping reactions.

I. Introduction

The kinetic rate laws of diffusion-limited elementary reactions in low dimensions have been shown to exhibit anomalous time dependences,[1−20] which are dramatically different from conventional rate laws found in many textbooks.[21] At the core of this anomalous kinetics behavior lies the fact that diffusion is not efficient enough to mix the reactants during reaction, resulting in the development of *self segregation* of the reactants in time. This self segregation leads to drastic reductions of the reaction rate and to other anomalous kinetic behaviors. It has also been shown by theory and simulations[2,5−9,12,20,22−24] that, in diffusion-limited reactions in low dimensions, there are regions called *depletion zones* where one species of the reactants is locally dominant with a corresponding depletion of the counter species in the region. The anomalous kinetic behavior has been predicted even in three dimensions (3D) for the elementary bimolecular reaction $A + B \rightarrow C$,[1,2,9] and this has been recently observed experimentally by Monson et al.[25]

A simple model with anomalous kinetic characteristics is the trapping reaction $A + T \rightarrow T$ in low dimensions, in which T is a static trap and A is a diffusing species that is annihilated upon collision with the trap. Following Smoluchowski,[26,27] one idealizes the reaction by assuming a single, immobile spherical T surrounded by an initially uniform distribution of A particles, each of which is allowed to diffuse, independent of the others, throughout an unbounded space. The occurrence of A−T reactions creates a zone of depletion around the trap, which is another form of self segregation of reactants. A quantitative characterization of this phenomenon can be framed in terms of one or more parameters. One of them is the rate of annihilation of the A species, R, which is predicted to be[28−30]

$$R \approx \begin{cases} t^{-1/2} & \text{for 1D} \\ \text{constant}/\ln(t) & \text{for 2D} \\ \text{constant} & \text{for 3D} \end{cases} \quad (1)$$

Lin et al.[31] tested this system by a photobleaching experiment for one dimension (1D) and two dimensions (2D), which demonstrated the dimensional dependence of the reaction rate for this system.

In this work, we attempt a direct experimental observation of the self segregation of reactants in an $A + T \rightarrow T$ system in an effectively 1D system. The kinetics of the growth of the depletion zone is examined with a new fluorescence-based setup. There are two parameters mainly used to describe the self segregation of reactants, which is equivalent to observing a depletion zone, quantitatively. One is the nearest-neighbor distance (usually denoted as $L(t)$), which is the distance from the trap (T) to the nearest "surviving" reactant (A) at a given time. Despite its significance and popularity from the theoretical point of view, this quantity would be extremely hard to measure directly in real experiments because of its molecular-level scale of magnitude, by definition. The other quantity, which is more manageable experimentally, is a "θ distance" (r_θ), the distance from the trap T to the point where the concentration of the reactants A reaches some specified fraction (θ) of it's value in the bulk. According to the theory by Havlin et al.,[29] the θ

† Part of the special issue "G. Wilse Robinson Festschrift".

* To whom correspondence should be addressed. E-mail: kopelman@umich.edu.

‡ University of Michigan.

§ E-mail addresses: parksh@umich.edu, peng@umich.edu, sparus@umich.edu, haimt@mail.biu.ac.il.

Bar-Ilan University.

10.1021/jp0141528 CCC: $22.00
Published on Web 04/11/2002

distance is predicted to show different *asymptotic* time scalings for a perfect trap in different spatial dimensions, that is,

$$\begin{aligned} r_\theta &\approx t^{1/2} && \text{in} \quad 1\text{D} \\ & t^{\theta/2} \quad (0 < \theta < 1) && \text{in} \quad 2\text{D} \\ & t^0 \quad (\text{“static”}) && \text{in} \quad 3\text{D} \end{aligned} \tag{2}$$

In our experiments, we measure the temporal changes in the spatial distribution of reactants inside and outside the trap. The experiment is the photobleaching of fluorescein dye molecules by a horizontally focused laser beam in a very shallow trough (150-μm thin cell). This also mimics an electrochemical setup in a very thin “sandwich” or wafer configuration with electrode side strips. The laser beam is focused in a *line shape* using a cylindrical lens to produce an effectively 1D environment. This experiment allows us to directly measure the θ distance and to compare with the theory described above. In the following, we will first describe the experimental procedures briefly and then present the data and the results of analyses. We also show that the experimental results are consistent with results from simulations and exact enumerations. We then perform a comparison study of the depletion zone behavior for different trap strengths. We find that there is an anomalous early-time regime for the growth of the depletion zone outside an imperfect trap, which has not been observed or predicted previously. We also show that the exact 1D lattice results carry over to quasi-1D systems for both perfect and imperfect trapping reactions. Finally, an equivalence of imperfect trapping in 1D system to the simple diffusion with radiation boundary condition is quoted and discussed.

II. Methods

1. Experimental Setup and Procedure. The experiment is the photobleaching of fluorescein dye molecules in a buffer solution using a focused laser beam. The photobleaching occurs inside a small gap between two flat microscope slides with dimensions 75 mm × 25 mm × 1 mm. Two optical fibers with a diameter of 150 μm are inserted as spacers between the two parallel microscope slides to produce a small gap with a thickness of 150 μm, which serves as a reaction vessel in this experiment. It has been shown recently[32] that the 150-μm gap between two flat microscope slides is small enough to provide a diffusion-controlled environment for the aqueous solutions without the presence of a gel, eliminating convection or any other mass-transport mechanism faster than diffusion. We made the reaction space as long as possible by positioning the two spacers 70 mm apart between the slides so as to minimize the possibility of finite size effects in the experiment. Fluorescein molecules were chosen for this experiment because fluorescein is well-known to be easily photobleached by intense excitation light sources.

The aqueous solution of fluorescein was prepared in a phosphate buffer solution at pH 8.5 with a concentration of 7×10^{-5} M. Spectroscopic grade fluorescein dye was purchased from Aldrich and used without further purification. The phosphate buffer solution was prepared by dissolving monobasic and dibasic potassium phosphate into triply distilled water. The buffer solution was used to increase the solubility of the fluorescein as well as to prevent any potential pH change of the solution during the photobleaching process. The aqueous fluorescein solution was injected into the 150-μm gap between two parallel slides using a glass pipet. After the sample was injected, a sealant (Krytox, DuPont Co.) was applied to the edges of the slides to prevent evaporation of the sample solution during the data acquisition.

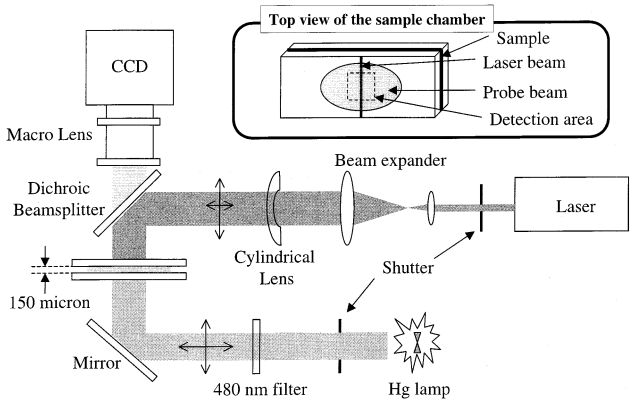

Figure 1. A schematic diagram of the experimental setup.

The experimental setup is depicted in Figure 1. We used a focused laser beam (“phototrap”) to photobleach the fluorescein dye molecules. The laser (see below) beam was expanded to approximately 1-in. diameter using two biconvex lenses and was then sent to a rectangular cylindrical lens ($f = 15$ cm) that focused the beam into a line shape, inside the sample plane, through a dichroic beam splitter unit. We put another focusing lens in front of the beam expander to reduce any loss of the laser power from the frequency doubler (see below), which produced a much more divergent beam than the argon-ion laser beam. The size of the focused laser beam in a line shape was ~60-μm wide and ~1-in. long on the sample plane. We used three different laser powers from two different wavelengths, at 488 and 430 nm, as the photobleaching laser beams to investigate the effect of the trap strength. A 488-nm line from an air-cooled Ar-ion laser (Ion Laser Technology, model no. 5490AWC-0), with 20 mW power at the output, served as the weak trap. A 430-nm femtosecond pulse from a frequency doubler (Spectra-Physics, model no. GWU-23FS) coupled with a Ti−sapphire laser (Spectra-Physics, Tsunami, model no. 3941-L1S) served as both a strong trap with 280 mW average output power and an intermediate trap with 210 mW average output power in the experiment. The laser powers at the sample position were 12 mW for the weak trap and 100 and 150 mW for intermediate and strong traps, respectively, producing more than a factor of 12 in intensity ratio between weak and strong traps. The power densities of the laser beams are calculated to be 7.9, 65.6, and 98.4 mW/mm^2 for weak, intermediate, and strong traps, respectively, at the focus on the sample plane.

Another light source at 480 ± 5 nm with approximately 1-in. diameter from a mercury lamp (Ushio, model no. USH-102D) was used to probe the progress of the photobleaching. The probe beam illuminates an elliptical area of 1-in. long horizontally and ~0.5-in. long vertically on the sample plane to generate fluorescence signals at different times, which are recorded by a detector. The power density of the probe beam from the mercury lamp on the sample plane is calculated to be less than 0.001 mW/mm^2, which is significantly smaller than the densities of the photobleaching laser beams described above. Hence, the effect of photobleaching by the probe beam can be neglected on the typical time scale of the entire experiment, which is less than 2 h. To support this argument, we prepared a sample solution in the same reaction vessel as the one that we used for the photobleaching experiments and illuminated with a probe beam, monitoring any signal drop in fluorescence emission caused from photobleaching by a probe beam. In this test, there

TABLE 1: Recursion Relationships of Reactant Concentrations at Position *i* (Integer) at Time $t = 0, 1, 2, \ldots$ for Various Line Trap Systems[a]

system	recursion relation	IC, $C(i,0)$	BC, $C(0,t)$
exact 1D, perfect trap	$C(i,t) = [C(i-1,t-1) + C(i+1,t-1)]/2$	C_0(const)	0
quasi-1D, perfect line trap	$C(i,t) = [C(i-1,t-1) + C(i+1,t-1)]/4 + C(i,t-1)/2$	C_0(const)	0
exact 1D, imperfect trap	$C(i,t) = [C(i-1,t-1) + C(i+1,t-1)]/2$	C_0(const)	$(1-p)[C(1,t-1)]$
quasi-1D, imperfect line trap	$C(i,t) = [C(i-1,t-1) + C(i+1,t-1)]/4 + C(i,t-1)/2$	C_0(const)	$(1-p)[C(1,t-1) + C(0,t-1)]/2$

[a] We assume the space and time to be discrete, and all of the particles are forced to move randomly at each time step. The trap location is 0. Quasi-1D means a 2D rectangular space where one edge is much longer than the other. IC = initial condition; BC = boundary condition; p = trap strength.

was no noticeable decrease in the fluorescence signal level at least for 2 h of continuous illumination, which verifies our argument. As a further protection to our sample from the probe beam, we put two computer-controlled mechanical shutters in front of two light sources to control the illumination times of the photobleaching laser beam and of the probe beam (mercury lamp) accurately during the photobleaching experiments. The shutters, coupled with a CCD detector, operate in such a way that the probe beam from the mercury lamp is illuminated on the sample only when the CCD camera takes a fluorescence image, while the photobleaching laser beam shines on the sample only when the photobleaching is underway and there is no data collection by the CCD. In this way, the probe beam is blocked during the photobleaching periods of the experiment and illuminates only during short data collection periods. This experimental design minimizes the total illumination time of probe beam on the sample to less than 3 min in the typical experiment, which collects 40 fluorescence images with a 4-s CCD integration time for each image recording.

The images of fluorescence emission from the sample were collected at different times, using a CCD camera (Spectra Source Instruments, model Teleris 2 12/16) equipped with a macro lens (Nikon, AF Macro 60 mm f2.8, 1:1). The CCD takes square images of size 1 cm × 1 cm with a 512 × 512 pixel resolution. Typical integration time of the CCD was 4 s for each image in the experiment.

After the sample solution in the reaction vessel was placed onto the sample holder, a probe beam at 480 ± 5 nm from the Hg lamp illuminated the entire area of detection, to generate the initial fluorescence signal. This fluorescence image was recorded (before the photobleaching laser beam was introduced) and was saved as an image at time $t = 0$. We use this image as a reference in the data analysis. To start the photobleaching, a laser beam was guided and focused onto the sample plane as a thin line, using the cylindrical lens. The beam was intense enough to start photobleaching within 1 s. After each bleaching time interval from 1 s in the beginning to 300 s in the final stage of the data collection period, the laser beam was blocked to stop bleaching during the CCD exposure time for taking the fluorescence image of the reactants at that time. The clock was stopped during this data-collection step, and the typical CCD exposure time in our experiments was 4 s. The photobleaching was followed for 1 h in the typical experiment. After photobleaching, we replaced the reaction vessel containing a photobleached sample solution with a new "sandwich" vessel containing only a phosphate buffer solution without fluorescein and took a blank image for the background correction in the data analysis. The home-built data acquisition program, which controls a CCD coupled with two shutters and time intervals between data acquisitions, allows us to measure time information accurately, which is especially crucial in the early time range, in which any small error is amplified and exaggerated in the logarithmic scale of the data analysis. The entire experiment is performed at room temperature.

In the data analysis, we first measured intensity profiles along one specific horizontal pixel line perpendicular to the laser beam trap from images at different times. Then, a background signal was subtracted and corrected, using a blank profile as well as the fluorescence intensity profile at time zero, which produced a spatial profile of the fraction of reactants surviving (θ) at a given time. The θ distances were measured at several different θ values directly from the fraction profiles for the different times and plotted in time on a log−log scale to measure the time scaling.

2. Simulations. Monte Carlo simulations were performed on a 200 × 200 square lattice, and a 200 × 2 line trap was put vertically in the middle of the lattice. Particles with the initial concentration 0.25 are randomly generated on the lattice at a time step zero. No more than one particle is allowed to occupy a given site at any moment, that is, we use the excluded volume principle. Particles are allowed initially to land, both inside and outside the trap, randomly. The diffusion is modeled by random walks at each time step of all particles (which are independent of each other). The cyclic boundary condition was used at the edges of the lattice. If a particle is chosen to move to a site that is already occupied by another particle, then this move is not allowed and the particle remains at its original site for that time step. If a particle moves into a trap site, it is trapped with a certain probability p. The effect of trap strength can be tested in the simulations by changing this trapping probability p from 0 (no trap) to 1 (perfect trap). The probability values tested in this work are $p = 0.01$, 0.02, 0.2, 0.8, and 1. Once the particle is trapped, it is removed irreversibly from the lattice, leading to a decrease in particle concentration. If it is decided that a particle is not trapped on the trap site, the particle continues to perform its random walk, just like all of the other particles. A concentration profile of reactants along the lattice at a given time step t was obtained by adding all of the particles in each column of the lattice parallel to the vertical trap at that time. Each simulation was run 100 times to achieve better statistics for the concentration profiles, except for the case of $p = 0.01$, which needed 1000 runs to get a satisfactory signal-to-noise (S/N) ratio. For all simulations, the reactant profiles were followed from 1 up to 900 time steps.

3. Exact Enumeration. We derived a series of recursive formulas for the A + T → T system with a static trap T in exact-1D and quasi-1D geometries. The equations are based on the lattice model[33] and generate the exact values of reactant concentrations, $C(i,t)$, at any position i at any time t for given initial and boundary conditions. The formulas are summarized in Table 1. Here, we describe briefly how the formula was derived for the simple case of the exact-1D system with a perfect trap. The idea can be easily extended to derive the formulas for the case of imperfect trap and for quasi-1D cases.

Consider an exact 1D lattice with a perfect trap of width 1 at position 0. All of the lattice sites outside the trap are equivalent, so particle A has the same probability to land on each lattice site. We use a constant C_0 ($0 < C_0 < 1$) to denote the initial

homogeneous probability, which is equivalent to the concentration of particles at each lattice site. Because the particles move randomly at each time step, we assume that the probability of one particle at position i at time t to move to the position $i - 1$ is the same as the probability to move to the position $i + 1$ at time $t + 1$. Hence, the concentration at the next time step $t + 1$ at position i can be described as

$$C_i(t+1) = [C_{i-1}(t) + C_{i+1}(t)]/2 \quad (3a)$$

The proper initial (IC) and boundary conditions (BC) should be

$$\text{IC:} \quad C_i(0) = C_0, \quad i = 1, 2, 3, ... \quad (3b)$$

$$\text{BC:} \quad C_0(t) = 0, \quad t = 0, 1, 2, 3, ... \quad (3c)$$

To check the validity of the recursion formulas in Table 1, we calculated and compared the concentration profiles with perfect trap for exact-1D and quasi-1D cases, which have a well-known scaling behavior of $t^{1/2}$. The numerical calculations were performed using the Matlab software package. The lattice size varied from 1000 to 3000 for the exact-1D system and was 1000 $\times$ 1000 for the quasi-1D system, and time steps were followed up to 10^4. The θ distances were measured from the calculated concentration profiles and plotted to see the time scaling. For the exact-1D system with imperfect trap, we used several different trap strengths (p) of 1 (perfect trap), 0.50, 0.20, 0.15, 0.10, 0.05, and 0.01. The time steps were followed up to 10^7 to achieve asymptotic behavior, and the lattice size was 3000.

III. Results and Discussion

1. Line Trap Experiments with Different Laser Beam Power. Figure 2 shows various fluorescence images from the experiment with a low photobleaching laser power, using the argon-ion laser. Figure 2a shows an image of the trap as a bright, thin vertical line in the middle, which is a focused laser beam on the sample plane. Figure 2b is a fluorescence image of fluorescein solution in the reaction vessel before photobleaching. This image is saved as data at time zero. Figure 2c shows the progress (in time) of the photobleaching of fluorescein by a laser beam. The images are background-corrected ones, using Figure 2b. The dark vertical band in the middle area of images represents the depletion zone outside the trap. The depletion zone appears to be dark because the photobleaching causes the fluorescein to be invisible to our detection system. We can see that the depletion zone grows continuously with time, as predicted by theory for 1D (as opposed to the case for the classical result in 3D in which the size of the depletion zone remains constant in time).

Figure 3 shows spatial profiles of the fraction (θ) of reactants surviving at different times obtained from experimental data for weak laser power in Figure 2. The plot shows the growth of the depletion zone in time quantitatively, enabling one to measure the θ distance directly. Similar fraction profiles were also obtained from the strong laser power experiments. We measured the θ distance at $\theta = 0.8$ from both experiments with different laser powers (see Figure 4). We notice a dramatic difference in the time scaling between the two data sets. The θ distance for the system with a strong laser power shows a $t^{1/2}$ behavior in the given time scale of the experiment, which is predicted as an asymptotic behavior for the perfect trap in 1D. However, the time exponent of the θ distance is clearly above $^1/_2$ for the system with weak laser power over the entire experimental time scale.

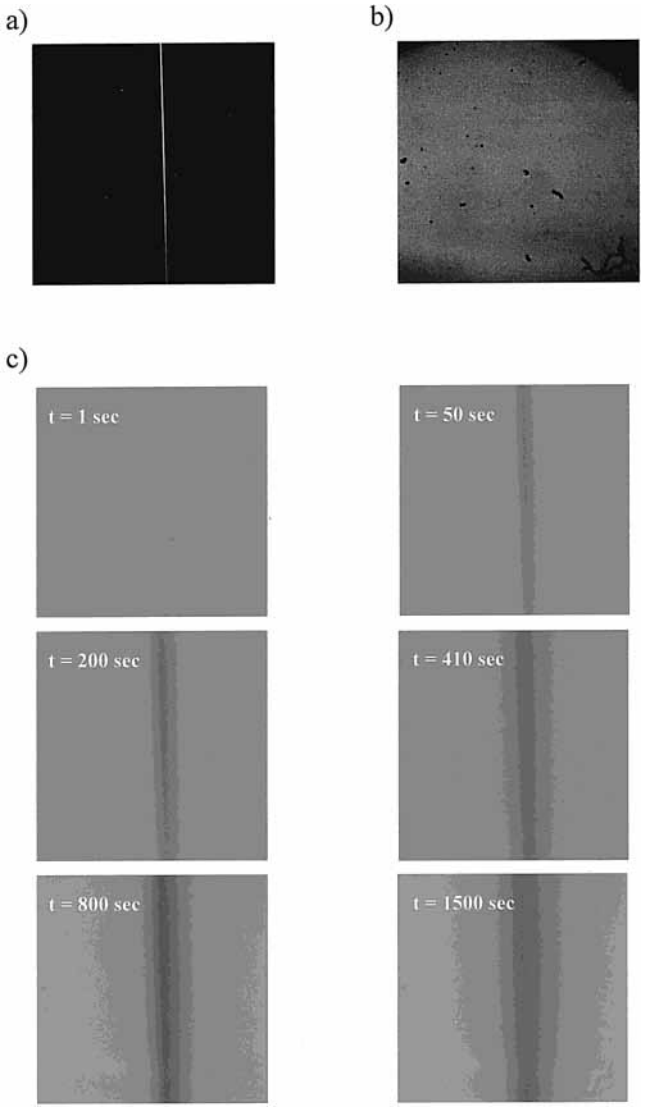

Figure 2. A typical line trap image (a) used for photobleaching. The laser beam is expanded and then focused into a line shape at the sample plane using a cylindrical lens ($f = 15$ cm). The trap width in this image is 60 μm. Fluorescence images of fluorescein without background corrections are shown (b) before photobleaching ($t = 0$) and (c) after $t = 1$, 50, 200, 410, 800, and 1500 s of photobleaching by line-shaped laser beam, after the background corrections using the image in panel b.

We believe that the different time scalings stem from the difference in photobleaching laser power, which corresponds to a difference in trapping strength, causing a slower approach to the asymptotic limit for the weak trap case. This result suggests that there should exist an early-time regime for weak traps, which is faster than the $t^{1/2}$ asymptotic behavior. It also suggests the existence of a crossover between the early-time and the asymptotic limit time regime for weak trap cases. To check this hypothesis, we performed the same photobleaching experiment with an intermediate laser power at 100 mW on the sample plane from the 430-nm pulsed laser. In Figure 4, we could see only the early-time behavior with a weak laser power and only the asymptotic behavior with a strong laser power. Therefore, by using an intermediate laser power for the trap, we expect to see both the early-time and the asymptotic-time regime within the time scale of the experiment. The θ distances were measured at $\theta = 0.8$ and 0.9 from the fraction profiles obtained from the experiment, which is shown in Figure 5. In this figure, the θ distances show a crossover from a fast,

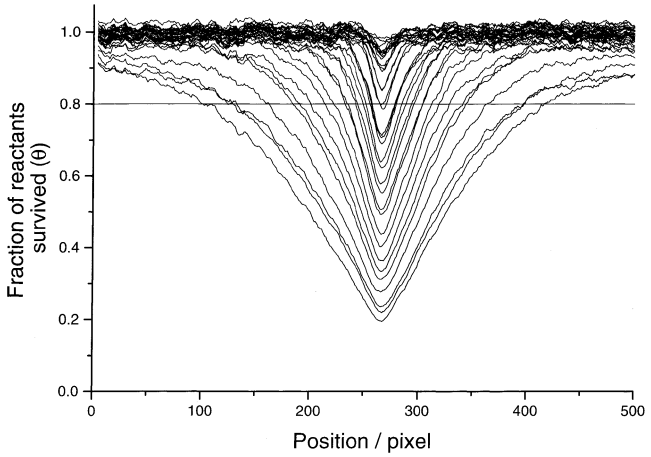

Figure 3. Typical background-corrected fluorescence intensity profiles along a horizontal pixel line across the line trap at different times from 1 s up to 2 h of photobleaching. The *y*-axis scale represents the fraction of reactants surviving at each position as the photobleaching progresses. Profiles are from the experiment using a trap with low laser intensity (Figure 2).

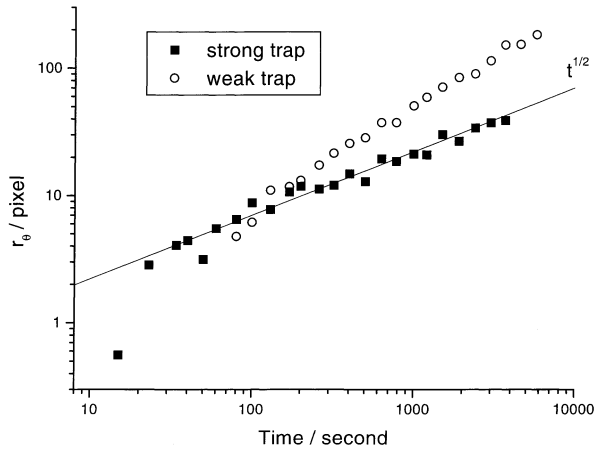

Figure 4. Plots of θ distance (r_θ) vs time from experiments. The r_θ's are measured at $\theta = 0.8$ for both the weak trap experiment with low laser intensity (profiles are shown in Figure 3) and the strong trap experiment with high laser intensity (profiles not shown). Note that we see the early time behavior up to ~2 h in the weak trap case, while the asymptotic regime is quickly achieved within 20 s in the strong trap case.

early-time behavior to the asymptotic $t^{1/2}$ behavior in the given time scale of the experiment, as expected. This result supports our argument that the trap strength affects the kinetics of the growth of the depletion zone around the trap, specifically for the time scaling of the θ distance in the early-time range, in an effectively 1D system. This hypothesis is tested and verified further by computer simulations and exact enumerations below.

2. Simulation: Effect of Trap Strength on Growth of Depletion Zone. The reactant profiles on a quasi-1D lattice at different times were obtained from Monte Carlo simulations for different trapping probabilities. A representative result for the trapping probability $p = 0.02$ is shown in Figure 6. All other simulation profiles for different trapping probabilities look very similar, except that a higher trapping probability causes a faster decrease in reactant concentration at the trap position on the lattice.

To obtain the scaling exponent, we measured θ distances at $\theta = 0.8$ for different probabilities and plotted against time on a log−log scale. The results are shown in Figure 7. The θ distance shows $t^{1/2}$ behavior for most of the time range for the

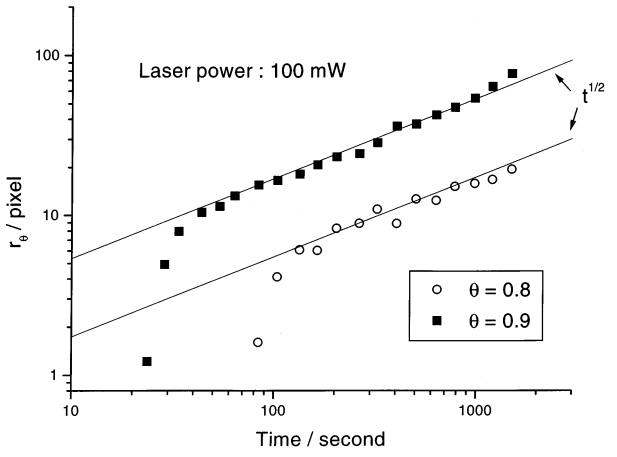

Figure 5. A plot of θ distance (r_θ) vs time from the experiment with an intermediate laser power. The r_θ was measured at $\theta = 0.8$ and 0.9 from the experimental data. Both data sets show a crossover behavior from the fast, early-time regime to the asymptotic, $t^{1/2}$ scaling regime.

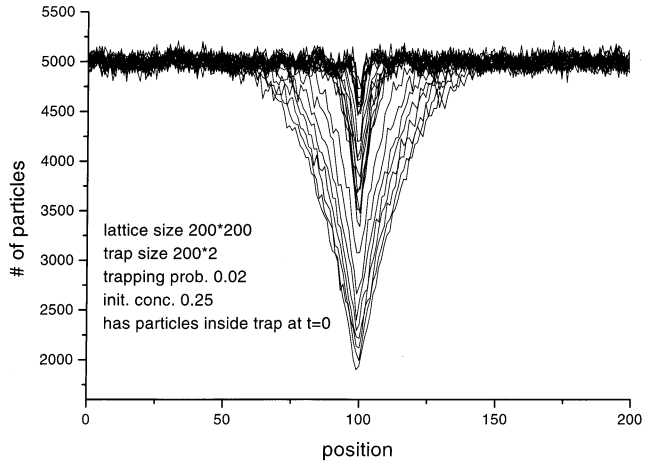

Figure 6. Spatial concentration profiles at different times up to 900 time steps for imperfect line trap in 2D from Monte Carlo simulation. The trapping probability, *p*, is 0.02 in this case. Simulations were performed on a 200 × 200 square lattice and a 200 × 2 line trap was put vertically at the center of the lattice. Initial particle density is 0.25. The cyclic boundary condition is used. Data are averaged 100 times for a better S/N ratio.

perfect trap with trapping probability 1 or 0.8, while there is an early-time regime with time exponent bigger than $^1/_2$ for trapping probabilities 0.2 or less. This directly supports our experimental result described earlier. Furthermore, it is shown that this early-time deviation lasts longer for a system with a lower trapping probability before it eventually converges to the asymptotic $t^{1/2}$ behavior.

3. Exact Enumeration. For a system in exact 1D with a perfect trap, the θ distances were measured at three different fractions ($\theta = 0.2$, 0.5, and 0.8) from the exact enumeration results for the concentration profiles, shown as solid lines in Figure 8, for time steps up to 10^4. The measured θ distances for different values of θ are plotted against time on a log−log scale in Figure 9 (filled symbols). The slopes are basically $^1/_2$ for the entire time range, regardless of θ. This result is well-known, but it confirms the validity of our recursion formula. There is a slight deviation of the slopes (0.49) from the theoretical value $^1/_2$, in early times, presumably due to the "discreteness" of our model for the mathematical equations.

The dotted line in Figure 8 is the exact concentration profile at a time step 10^4 for the quasi-1D system, with a perfect "line"

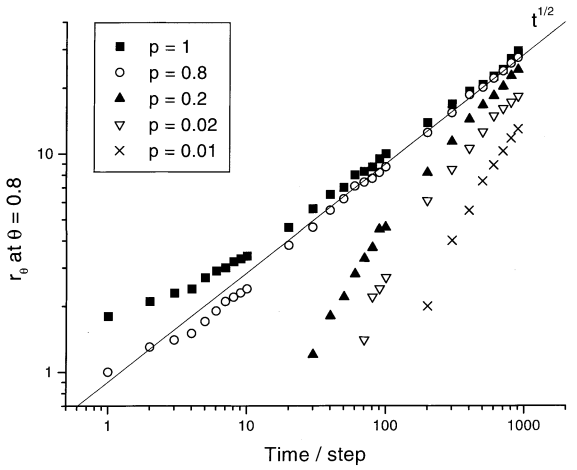

Figure 7. A plot of r_θ vs time at $\theta = 0.8$ from Monte Carlo simulations. Trap strength (p) is varied between 1 (perfect trap) and 0.01. Each simulation was averaged 100 times to achieve a decent S/N ratio, except for the case of $p = 0.01$, which was averaged 1000 times to obtain a reasonable S/N ratio. Note the more dramatic effect of early time behavior as the trap strength decreases.

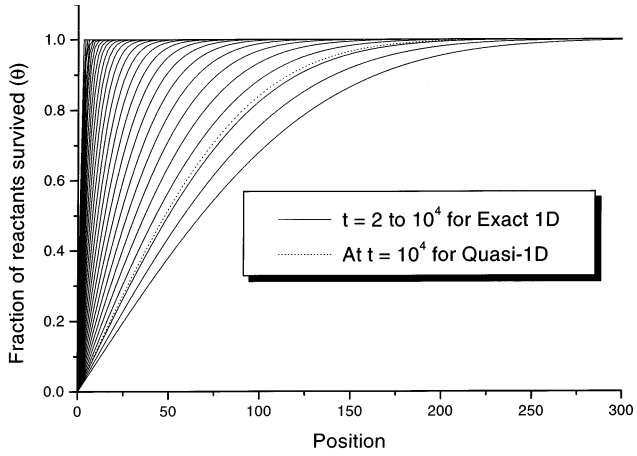

Figure 8. The reactant concentration profiles at different times from exact enumeration calculations for a perfect trap in exact 1D (solid lines). The trap is located at position 0, and the trapping probability is $p = 1$. The time step is up to 10^4. Similar concentration profiles can be obtained for a perfect trap in quasi-1D, in which the trap is located vertically at the edge of the 3000×3000 square lattice. For comparison, only one concentration profile at a time step 10^4 for the quasi-1D case is shown as a dotted line in this figure. Calculations were performed on Matlab.

trap lying on a 2D lattice. For the quasi-1D system, we notice that the overall diffusion distance is much shorter than for the exact 1D case. This is well expected because particles can now move in perpendicular directions as well as in horizontal directions on the 2D lattice. However, the time exponents of the θ distance at different θs, shown as open symbols in Figure 9, are basically the same as in the exact 1D case, that is, $^1/_2$ in the entire time range of up to 10^4 steps. This result shows that a perfect line trap on a 2D plane actually generates an effective 1D behavior for the reactant profiles, which supports our basic assumption in this work. This result also suggests that we can simply use an exact-1D model to study a scaling behavior for a quasi-1D system.

Now we discuss the results for the quasi-1D system with an imperfect trap, which closely corresponds to our experimental system. On the basis of the conclusion that the scaling results are identical for the exact-1D and quasi-1D system for the perfect trap, we simply used the formula for the exact 1D with

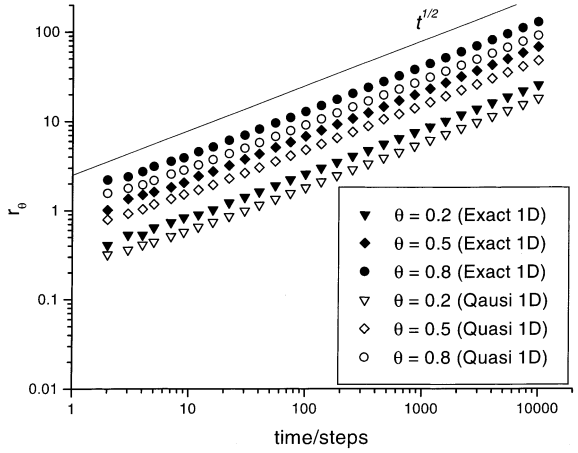

Figure 9. A plot of r_θ vs time for the perfect trap in exact 1D (filled symbols) and in quasi-1D (open symbols) from exact enumerations. The θ distances are measured at $\theta = 0.8$, 0.5, and 0.2.

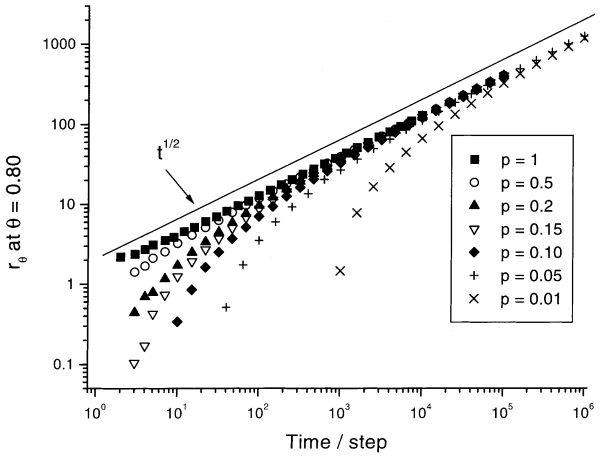

Figure 10. A plot of r_θ vs time for various trap strengths in 1D from exact enumerations. The θ distances are measured at $\theta = 0.8$ for all different trap strengths. Note that there is an early-time regime for weak traps, while the perfect trap has no such behavior. Also Note that all of the θ distances at different trap strengths eventually converge to the 1D $t^{1/2}$ behavior at the long-time limit.

imperfect trap in this case. This allows us to study a much longer time scale, which is crucial for observing the asymptotic behavior for the imperfect trap system. A series of reactant concentration profiles, similar to those in Figure 8, were obtained for different trapping probabilities from the exact enumeration calculations for an imperfect trap in 1D. We measured the θ distances from the profile and plotted them in time, as shown in Figure 10. We see that they all converge to the one-dimensional $t^{1/2}$ behavior at the long-time limit, with anomalous early-time deviations observed only for the imperfect traps. The present result matches well with the experimental as well as the simulation results for the imperfect trap systems in quasi-1D.

It is interesting to note that, according to Ben-Naim et al.,[34] the infinite 1D trapping system with an imperfect trap is equivalent to a semiinfinite 1D free diffusion system with a radiation boundary condition. From this equivalence, an exact expression for the concentration of the reactants for imperfect trap in 1D is the same as the solution for the diffusion equation in semi-1D with radiation boundary condition, which is[33−35]

$$c(x,t) = c_0\{\mathrm{erf}[x/(4Dt)^{1/2}] + \exp(\kappa^2 Dt + \kappa x)\,\mathrm{erfc}[(x + 2\kappa Dt)/(4Dt)^{1/2}]\} \quad (4)$$

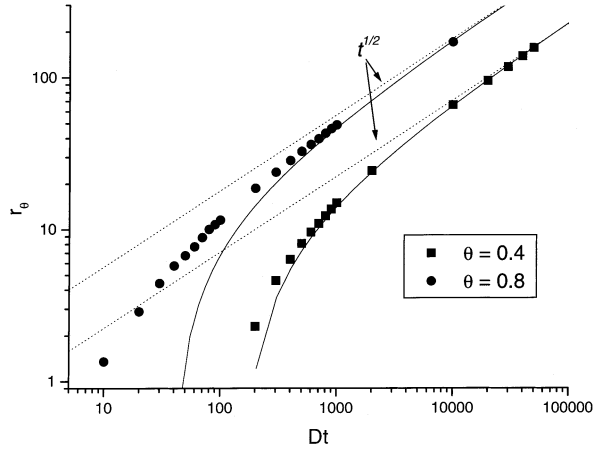

Figure 11. A plot of r_θ vs time for a trap strength $\kappa = {}^1/_9$ in exact 1D from exact solution. The θ distances were measured at $\theta = 0.8$ (●) and 0.4 (■). The solid lines represent the fit of the data with eq 5.

where c_0 is the initial reactant concentration, D is a diffusion constant of the reactant, κ is an absorption rate of the trap, which is defined to be zero for complete reflection (no trapping) and ∞ (infinity) for perfect trapping. The erf(z) is the error function and erfc(z) is the complementary error function. We generated a series of concentration profiles for $\kappa = {}^1/_9$ using this equation, and the θ distances were measured for $\theta = 0.4$ and 0.8, which are shown as circles and squares in Figure 11. At *sufficiently* long time, the expression of r_θ can be approximated from eq 4 as[35]

$$r_\theta \cong \theta \sqrt{\pi D t} - 1/\kappa \qquad (5)$$

According to this result, when the trap is imperfect, the asymptotic $t^{1/2}$ behavior for r_θ is recovered after a *very* long time, where $\theta\sqrt{\pi D t} \gg 1/\kappa$. However, r_θ deviates from the $t^{1/2}$ scaling when the time is not long enough and the effect of the second term ($1/\kappa$) in eq 5 is not negligible. Therefore, eq 5 holds for both asymptotic $t^{1/2}$ range and a *marginally long* time range (say, an "intermediate"-time range), where r_θ deviates from the asymptotic $t^{1/2}$ scaling. The solid lines in Figure 11 are an attempt to fit the analytical data for the θ distances from eq 4 with the long-time approximation in eq 5. The solid lines collapse at a short-time range, but fit well with the slight deviations from the $t^{1/2}$ behavior at an "intermediate" time range as well as with the asymptotic $t^{1/2}$ behavior. This partially explains the anomalous early-time deviations of the θ distance from asymptotic behavior for the imperfect trap systems in Figures 4, 5, 7, and 10.

IV. Summary

The effect of trap strengths on the growth of depletion zones in A + T → T with a static trap T in 1D was studied. Different trap strengths were achieved by changing the laser power (served as a phototrap in the experiment). The strong laser power simulated a perfect trap, which has a $t^{1/2}$ scaling behavior for the θ distance over most of the time range. However, the experiment with a weak laser power produced an anomalous early-time behavior for the θ distance, which is faster than the $t^{1/2}$ scaling. A crossover behavior from the early-time regime to the asymptotic-limit regime was observed experimentally, using an intermediate strength laser power. The experimental results are consistent with an exact one-dimensional analytical solution and were also reproduced in the computer simulations as well as by the exact enumeration calculations. A simple, quasi-1D, imperfect trapping model is consistently corroborated by the experiments, the simulations, and the exact enumerations. The new fluorescence-based experimental system enables the simultaneous spatial and temporal resolution required for this study.

Acknowledgment. We thank Mr. Rodney Agayan for technical help with Matlab calculations. We also thank Prof. Panos Argyrakis for helpful comments and discussions on this work. We appreciate useful suggestions by Dr. Yong-Eun Lee Koo on this manuscript. Support from NSF Grant DMR 9900434 is gratefully acknowledged.

References and Notes

(1) Ovchinnikov, A. A.; Zeldovich, Y. B. *Chem. Phys. B* **1978**, *28*, 215.
(2) Toussaint, D.; Wilczek, F. *J. Chem. Phys.* **1983**, *78*, 2642.
(3) Meakin, P.; Stanley, H. E. *J. Phys. A* **1984**, *17*, L173.
(4) Kang, K.; Redner, S. *Phys. Rev. Lett.* **1984**, *52*, 955.
(5) Kang, K.; Meakin, P.; Oh, J. H.; Redner, S. *J. Phys. A* **1984**, *17*, L665.
(6) Kang, K.; Redner, S. *Phys. Rev. A* **1985**, *32*, 435.
(7) Lindenberg, K.; Romero, A. H.; Sancho, J. M. *Int. J. Bifurcation Chaos* **1998**, *8*, 853.
(8) Leyvraz, F.; Redner, S. *Phys. Rev. Lett.* **1991**, *66*, 2168.
(9) Kopelman, R. *Science* **1988**, *241*, 1620.
(10) Havlin, S.; Benavraham, D. *Adv. Phys.* **1987**, *36*, 695.
(11) Clement, E.; Kopelman, R.; Sander, L. M. *Europhys. Lett.* **1990**, *11*, 707.
(12) Lindenberg, K.; Argyrakis, P.; Kopelman, R. *J. Phys. Chem.* **1995**, *99*, 7542.
(13) Sibona, G. J.; Budde, C. E.; Condat, C. A. *Phys. Rev. E* **1996**, *54*, 6232.
(14) DominguezAdame, F.; Rodriguez, M. A.; Sanchez, A. *Phys. Lett. A* **1997**, *227*, 381.
(15) Condat, C. A.; Sibona, G. J.; Budde, C. E. *J. Stat. Phys.* **1997**, *89*, 369.
(16) ben-Avraham, D. *Phys. Rev. E* **1998**, *58*, 4351.
(17) Schlipf, S.; Katori, H.; Perotti, L.; Walther, H. *Opt. Express* **1998**, *3*, 97.
(18) Makhnovskii, Y. A.; Berezhkovskii, A. M. *Chem. Phys. Rep.* **1999**, *18*, 103.
(19) Kirsch, A. *Int. J. Mod. Phys. C* **1999**, *10*, 753.
(20) Taitelbaum, H.; Koza, Z. *Physica A* **2000**, *285*, 166.
(21) For example, see: Atkins, P. *Physical Chemistry*, 6th ed.; W. H. Freeman & Co.: New York, 1998.
(22) Kopelman, R.; Parus, S. J.; Prasad, J. *Chem. Phys.* **1988**, *128*, 209.
(23) Peacock-Lopez, E.; Keizer, J. *J. Chem. Phys.* **1988**, *88*, 1997.
(24) Argyrakis, P.; Kopelman, R.; Lindenberg, K. *Chem. Phys.* **1993**, *177*, 693.
(25) Monson, E.; Kopelman, R. *Phys. Rev. Lett.* **2000**, *85*, 666.
(26) Smoluchowski, M. V. *Z. Phys. Chem.* **1917**, *92*, 129.
(27) Rice, S. A. *Diffusion-Limited Reactions*; Elsevier: Amsterdam, 1985.
(28) Weiss, G. H.; Kopelman, R.; Havlin, S. *Phys. Rev. A* **1989**, *39*, 466.
(29) Havlin, S.; Larralde, H.; Kopelman, R.; Weiss, G. H. *Physica A* **1990**, *169*, 337.
(30) Taitelbaum, H.; Kopelman, R.; Weiss, G. H.; Havlin, S. *Phys. Rev. A* **1990**, *41*, 3116.
(31) Lin, A. L.; Monson, E.; Kopelman, R. *Phys. Rev. E* **1997**, *56*, 1561.
(32) Park, S. H.; Parus, S.; Kopelman, R.; Taitelbaum, H. *Phys. Rev. E* **2001**, 64, 055102 (R).
(33) Carslaw, H. S.; Jaeger, J. C. *Conduction of Heat in Solids*, 2nd ed.; Clarendon: Oxford, U.K., 1959.
(34) Ben-Naim, E.; Redner, S.; Weiss, G. H. *J. Stat. Phys.* **1993**, *71*, 75.
(35) Taitelbaum, H. Ph.D. Thesis, Bar-Ilan University, Ramat-Gan, Israel, 1991.